

CALIBRATION OF A FLUID FOR USE  
IN THE AQUARIUM TECHNIQUE  
FROM -45 TO +165 F

C. E. Canada

DEVELOPMENT DIVISION

APRIL - JUNE 1971

Normal Process Development  
Endeavor No. 236

**MASTER**

DISTRIBUTION OF THIS DOCUMENT IS UNLIMITED *dg*



*Mason & Kanger - Silas Mason Co., Inc.*  
*Portex Plant*

P. O. BOX 647  
AMARILLO, TEXAS 79105  
806-335-1581

operated for the  
ATOMIC ENERGY COMMISSION  
under  
U. S. GOVERNMENT Contract DA-11-173-AMC-487 (A)

**DISCLAIMER**

**Portions of this document may be illegible  
in electronic image products. Images are  
produced from the best available original  
document.**

**NOTICE**

**This report was prepared as an account of work sponsored by the United States Government. Neither the United States nor the United States Atomic Energy Commission, nor their employees, nor any of their contractors, subcontractors, or their employees, makes any warranty, express or implied, or assumes any legal liability or responsibility for the accuracy, completeness or usefulness of any information, apparatus, product or process disclosed, or represents that its use would not infringe privately-owned rights.**

CALIBRATION OF A FLUID FOR USE IN THE AQUARIUM TECHNIQUE  
FROM -45 TO +165 F

*C. E. Canada*

DEVELOPMENT DIVISION

The purpose of this project is to extend the present aquarium technique to encompass the temperature range from -45 to +165 F by selecting and calibrating an applicable fluid.

April - June 1971  
Normal Process Development  
Acct. No. 22-2-44-01-236  
Endeavor No. 236

Section T

# CALIBRATION OF A FLUID FOR USE IN THE AQUARIUM TECHNIQUE FROM -45 TO +165 F

## ABSTRACT

The aquarium technique has been extended to encompass the temperature range from -45 to +165 F by selection and calibration of a dimethyl polysiloxane fluid suitable for the referenced range.

Results are given for the Hugoniot, and techniques used in selection and calibration are discussed.

## DISCUSSION

In general, the distance-time history of a shock front moving through a transparent medium is obtained by the "aquarium" technique. Differentiation of the distance-time curve yields shock velocity information, and given the Hugoniot of the transparent medium, a pressure-time history may be calculated.

Distilled water typically comprises the transparent medium for the aquarium technique, hence, desirable properties of the fluid to be selected were patterned after those of water.

Following is a list of more obvious properties required of the fluid:

1. In each of the applications discussed above, the fluid must remain optically transparent over the required temperature range.
2. In order to avoid calculational and experimental uncertainties, the fluid should not have elastic or phase transitions over the temperature and pressure ranges of interest.
3. Use of aquarium technique for timing and output pressure information only requires a compressible fluid with a known equation-of-state. Additional requirements are imposed when using the fluid for equation-of-state determinations. For example, Hugoniot may be obtained by the Hugoniot reflection method(1), in which samples of interest are immersed in the fluid and subjected to various shock pressures. Measurements of a range of shock velocities incident on the material and corresponding transmitted shock velocities together with a knowledge of the mass density of the sample and Hugoniot of the fluid, are sufficient to determine the Hugoniot for the material of interest.

The Hugoniot reflection method is based on the approximation that the shocked state of the immersed sample lies on the  $(P, UP)$ -curve defined by a translated, mirror image of the fluid's Hugoniot. This approximation is valid provided the shock impedances of the two materials are such that the incident and transmitted Hugoniot states are close together in the  $(P, UP)$ -plane.

By selecting a material with properties similar to distilled water, materials that may be investigated are limited to those that may also be examined using water.

4. Fluid should be chemically inert, non-flammable and non-toxic for ease of handling, and compatible with anticipated materials.
5. Electrical properties should be similar to those of water.
6. Chemical composition of the fluid should be as simple as possible to permit theoretical predictions and calculations.
7. The fluid should be relatively inexpensive consistent with the above.

#### EXPERIMENTAL TECHNIQUES AND RESULTS

The search for a suitable fluid consisted of two phases. First a literature survey of frequently reported fluid properties, such as thermal, chemical and optical characteristics was undertaken. Numerous materials were quickly rejected during the first phase since they did not satisfy all of the requirements.

Fluids remaining under consideration after the first phase and those subjected to further testing included the Du Pont Freons<sup>a</sup>, E-3 and E-5, a solution of ethylene glycol and water, and low viscosity, dimethylpolysiloxanes<sup>b,c</sup> (silicone fluids).

The second phase involved investigation of low pressure shock characteristics at room temperature and optical properties from -65 to +165 F.

Qualitative low pressure characteristics were obtained by exploding wires in the fluids and monitoring the resulting shock velocity curve. These tests determined if the fluids partially satisfied, at low pressure, requirement [3] as listed in the previous section.

Optical properties of the fluids were examined by measuring the photographic resolution of objects imaged through the fluids.

DuPont Freon fluids were excluded from consideration at this point. These Freons, although exhibiting the desired properties, were substantially higher in cost/weight.

---

<sup>a</sup>E. I. DuPont DeNemours & Company, Inc., Technical Bulletin EL-8A.

<sup>b</sup>General Electric, Technical Bulletin S-90.

<sup>c</sup>Union Carbide Technical Bulletin, "Engineering with Silicone Fluids", 1971, L-45, 7 Centistokes.

Qualifying, room temperature Hugoniot over a limited pressure range were next determined for the fluids left in consideration. Aquariums were used for these tests. They were constructed from PMMA<sup>d</sup> with dimensions of 4 x 4 x 2 in. Four 1/8-inch thick plates of PMMA were equally spaced across the 2-inch dimension and the remaining space was filled with the fluid to be tested. Shock velocities, produced by plane wave generators, incident on and transmitted thru the PMMA plates were monitored with a streak camera, a record of which is shown in Fig. 1.

Based on the tests described above, L-45 was selected for Hugoniot evaluation.

Calibration was accomplished using a modification of a technique described by D. V. Keller(2). A schematic of the testing configuration is shown in Fig. 2 while Fig. 3 shows a resulting streak camera record.

Pre-alignment of the lighting and optical systems was accomplished with a simulating aquarium. Then the actual aquarium was removed from its thermal environment, inserted in place of the simulator, and tested within four to seven minutes.

Temperature-time curves for the L-45 fluid, with time referenced to removal of the aquariums from their environments, are shown in Figs. 4 and 5. Two thermocouples, one located near the reflection surface (closed circles) and one near an outside surface (open circles), were used for these data. In order to test at desired temperatures the aquariums were conditioned from -50 to -55 F and from +170 to +175 for the cold and hot environments respectively.

Prior to emergence of the shockwave from surface A, both direct and reflected images of scribed lines C and D and reflected images of B are discernible. (See Fig. 3).

After breakout from A, but before the front impacts C, surface A moves at particle velocity  $UP(1)$ , characteristic of the fluid, whereas shadows of B, C, and D as measured by the streak camera, move at velocity  $U(1)$  dependent on  $UP(1)$ . Direct images of C and D appear stationary during this time period.

After the shock front impacts C, but prior to its reaching D, the surface described by C moves at particle velocity  $UP(2)$  characteristic of the PMMA. The reflected images of B and D continue at  $U(1)$ , but now the direct image of C appears to move at  $U(2)$  whereas its shadow moves at  $U(3)$ , which depends on the difference  $[UP(1) - UP(2)]$ .

When the shock front reaches D the surface moves with particle velocity  $UP(3)$ , characteristic of the fluid. The direct image of D now appears to move at  $U(4)$ , whereas the shadow of D appears to move at  $U(5)$ , which depends on the difference  $[UP(1) - UP(3)]$ .

Shock velocities corresponding to the various observed surface velocities obtain from time differences at which the scribed lines move and a previous knowledge of the geometry.

---

<sup>d</sup>Rohm & Haas, Plexiglas G, Data Sheet PL-229K

2 msec

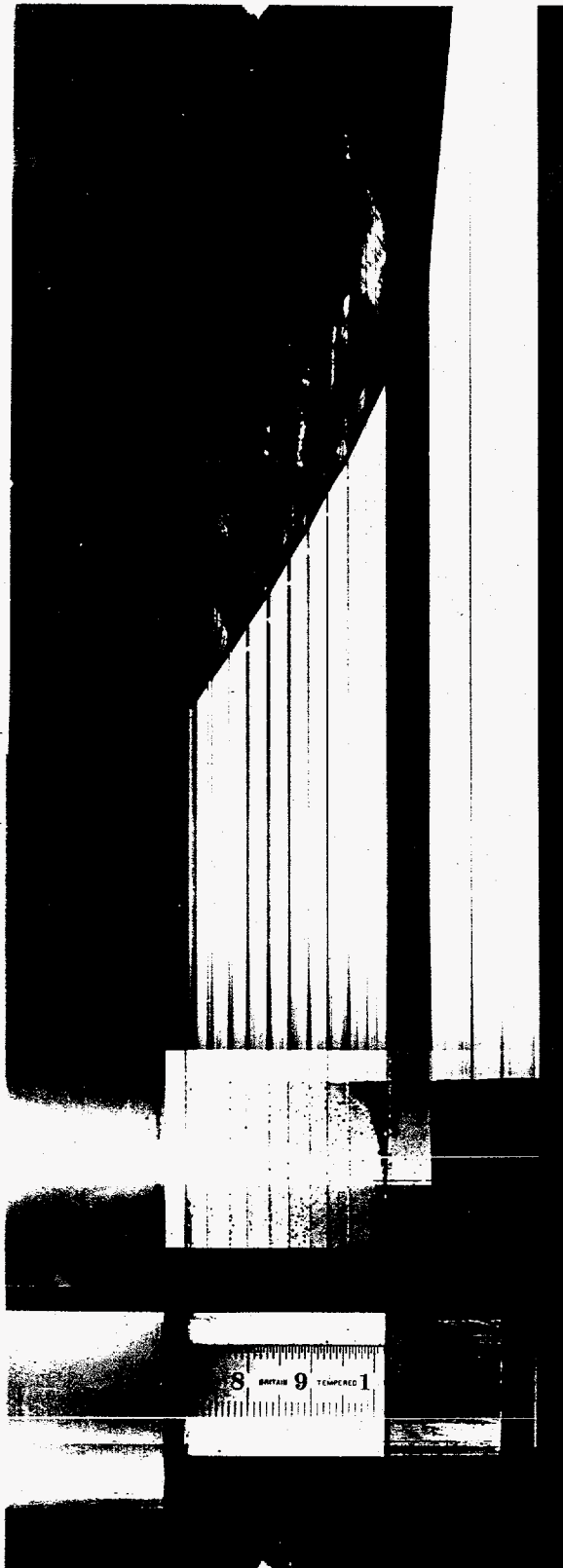
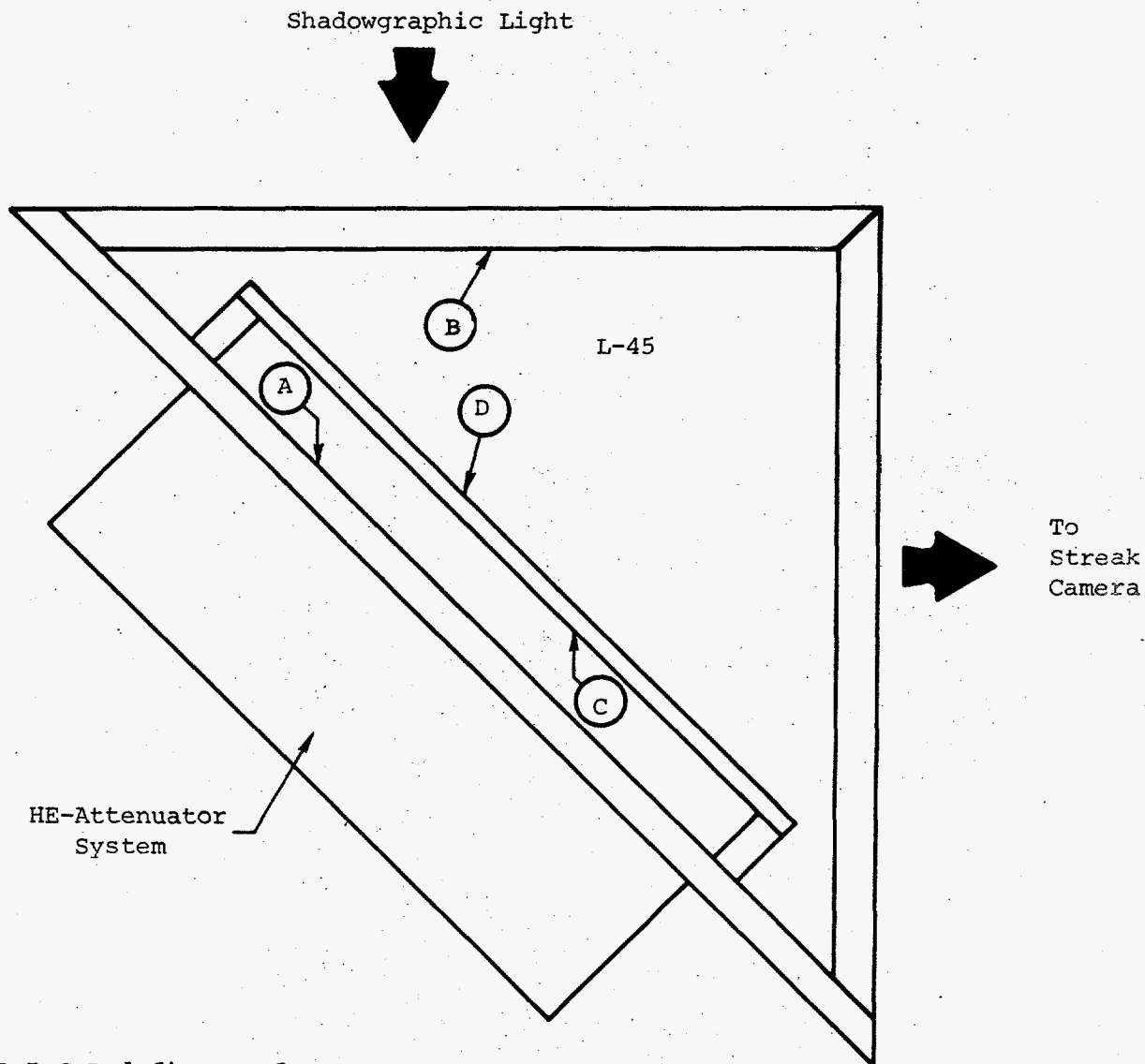


Fig. 1. Streak Record for Low-Pressure, Qualifying Hugoniot





1. A,B,C,D define surfaces.
2. A is a reflective, vacuum deposited, aluminum surface.
3. Scribed lines are applied to B,C,D.
4. Distance from A to C: 1/8-inch.
5. Distance from C to D: 1/16-inch.
6. Aquarium constructed with PMMA.

Fig. 2. Sketch of Prism Aquarium, System

| 2  $\mu$ sec |



Fig. 3. Typical Streak Record for Calibration of L-45 Fluid

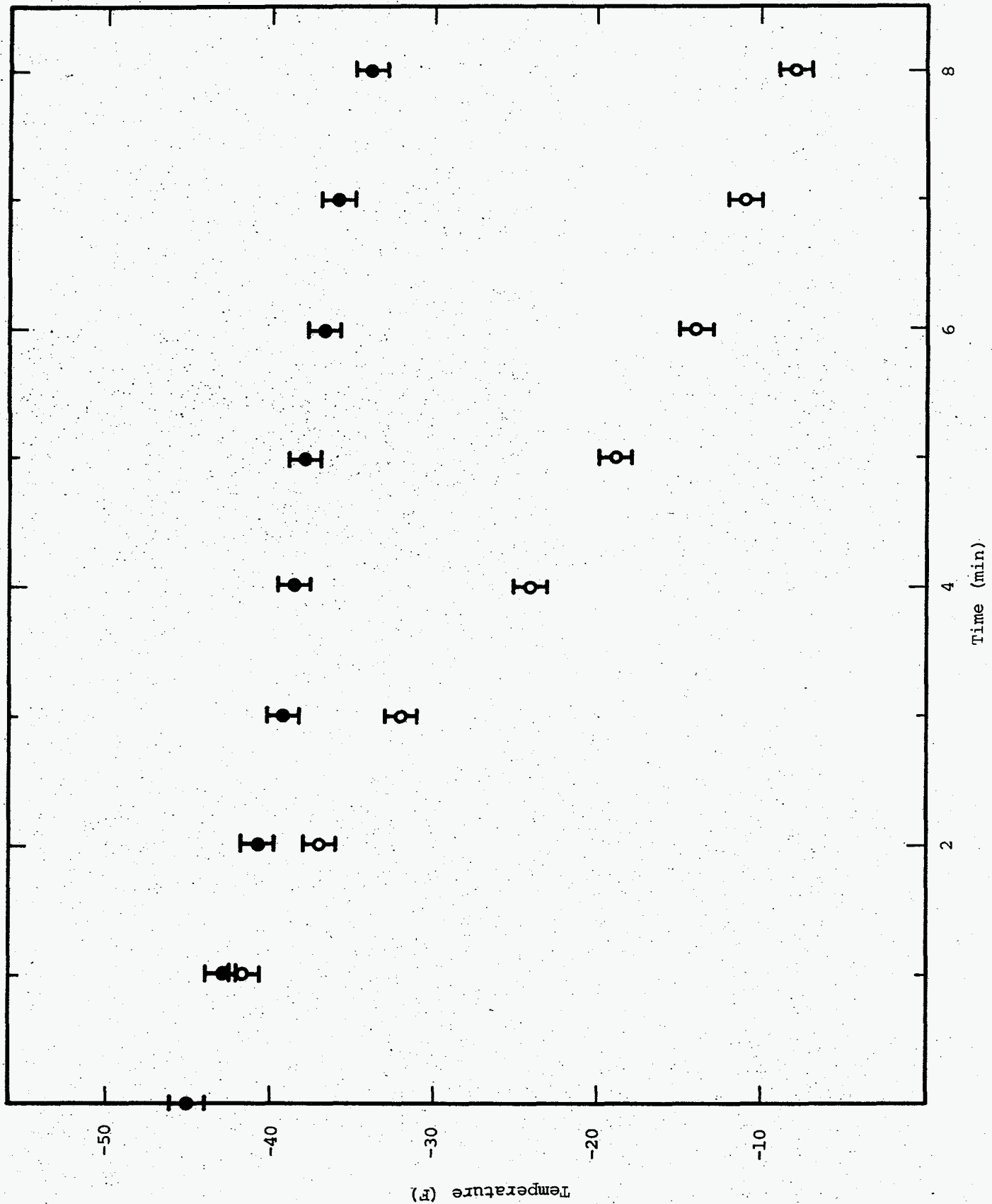


Fig. 4. Temperature-Time Curves for L-45 Fluid Conditioned at -45 F

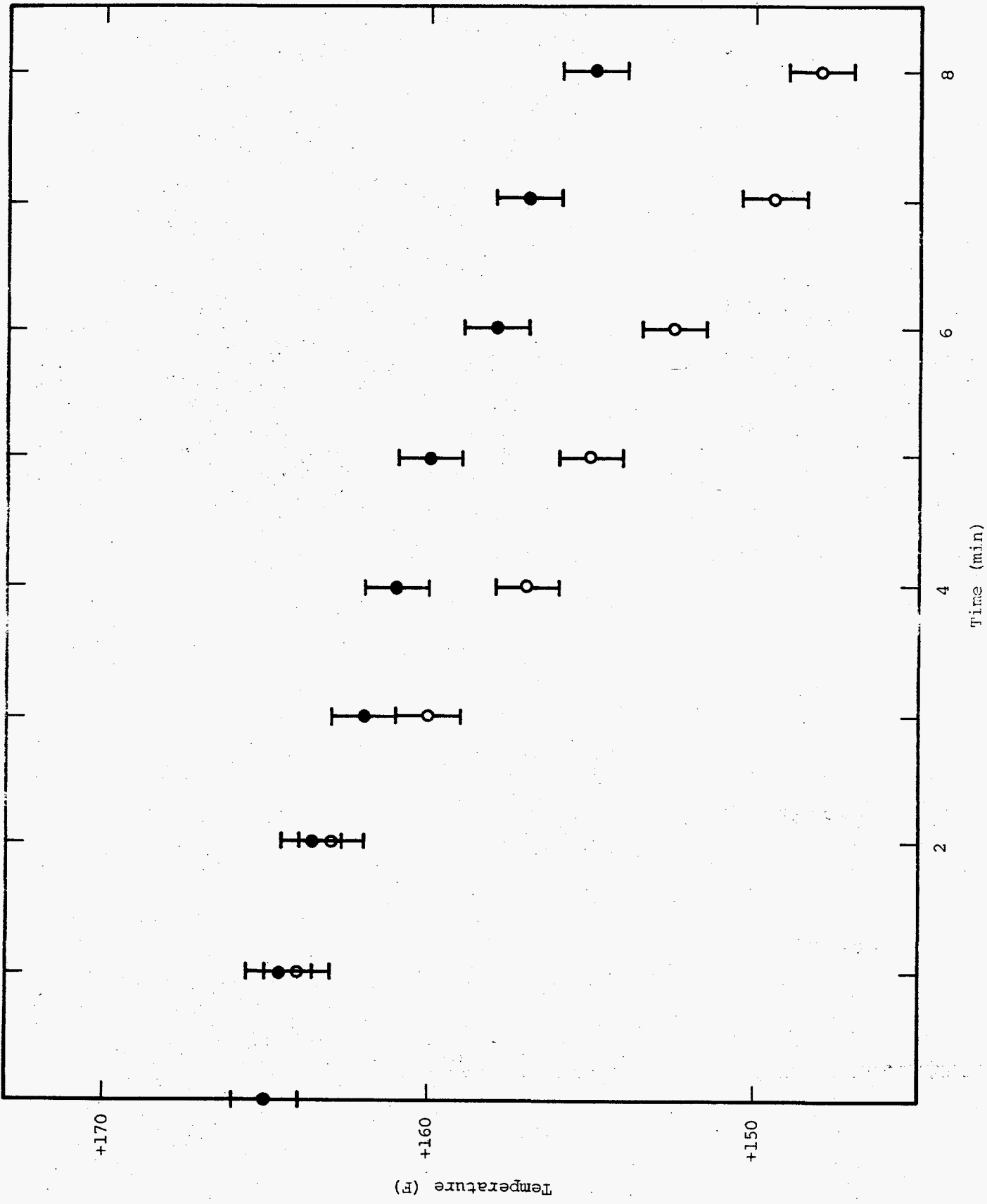


Fig. 5. Temperature-Time Curves for L-45 Fluid Conditioned at +165 F

Of the features discussed above, U(1) and US(1) obtained from the difference in time between initial motion of surfaces A and C are sufficient to determine the Hugoniot of L-45.

In addition, the Hugoniot of PMMA is in principle derivable from U(2), U(3), and the difference in time between initial motions of C and D [US(2)]. However, resolution did not permit accurate measurements of U(2) and U(3), so the Hugoniot was calculated using the Hugoniot reflection method.

The Hugoniots of L-45 based on U(1) data are the main goal of the project. The PMMA-data obtained from the test geometry were secondary.

Observed surface velocities discussed above are tabulated in Table I. Conversion of these velocities to particle and shock velocities depend on geometry, local index of refraction and separation of the shock front from the various surfaces.

Passage of the shock front imparts motion to the various surfaces described above. However, the apparent position of the scribed lines is shifted from the real location due to the index of refraction change behind the shock front. Fig. 6 illustrates the effect and indicates necessary calculations. A plane wave profile with a step increase in index of refraction behind the shock front is assumed. The refractive index behind the shock front is denoted by N(r) while that in front is denoted by N(i).

As can be seen in Fig. 6, the angles between the optical axis and surface normals were 45 degrees for all tests conducted.

Observed surface velocities are related to particle velocities as follows:

$$U(1) = \sqrt{2} * [UP(1) * \tan(r) + US(1) * (1 - \tan(r))] \quad (1)$$

where r, the angle of refraction, depends on the index of refraction through Snell's Law,

$$N(r) * \sin(r) = N(i) * \sin(i), \quad (2a)$$

$$\text{and } \tan(r) = \left[ \sin(r) \right] / \left[ 1 - \sin^2(r) \right]^{1/2} \quad (2b)$$

where i is the incident angle.

The Gladstone-Dale model [3] predicts,

$$\left[ N(r) - 1 \right] / \rho = K \quad (3)$$

where  $\rho$  is mass density and K is a constant dependent on initial value of N and  $\rho$ . Further  $\rho$  is related to US and UP by

$$\rho_0 * US = \rho * \left[ US - UP \right] \quad (4)$$

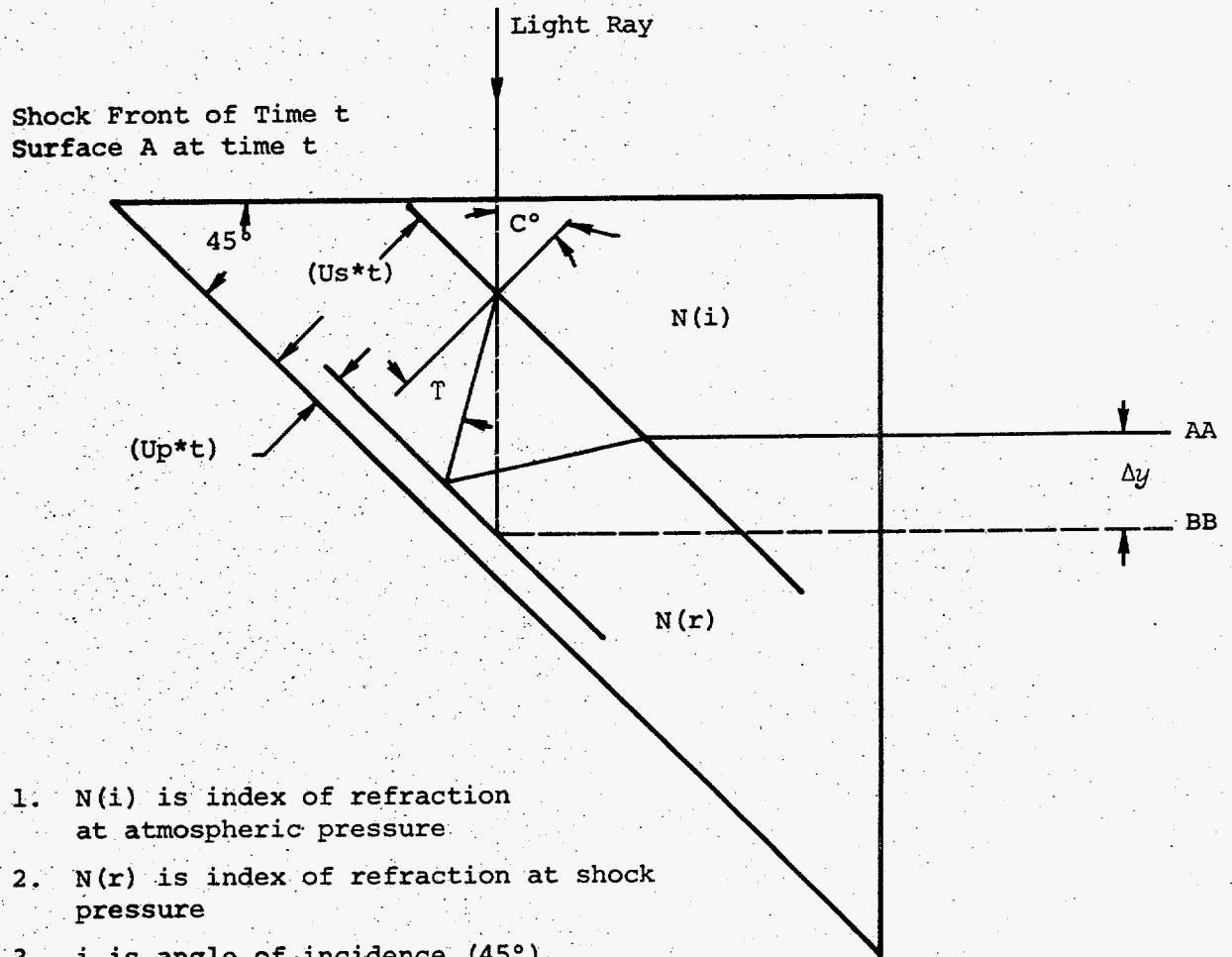
where  $\rho_0$  is initial mass density.

Table I. Measured Shock and Surface Velocities

Temperature* (° F)	U(1) (mm/μsec)	US(1)** (mm/μsec)	US(2) (mm/μsec)
R.T.	0.000	0.991	————
R.T.	1.170	2.019	————
R.T.	2.351	3.218	4.036
R.T.	3.091	3.760	4.485
R.T.	4.964	5.655	5.961
-45	0.000	1.175	————
-45	1.544	2.575	3.633
-45	1.881	3.018	3.647
-45	2.140	3.350	4.230
-45	3.594	4.266	4.587
-45	4.551	5.452	5.494
-45	4.909	6.071	6.028
+165	0.000	0.825	————
+165	1.449	2.065	3.356
+165	1.557	2.302	2.828
+165	1.794	2.768	3.497
+165	2.236	2.762	3.905
+165	2.919	3.497	————
+165	4.878	5.274	5.787

\* R.T. ranged between 76 to 87 F.

\*\*Values for US(1) at U(1) equal to zero were obtained from exploding wire generated waves in L-45.



- Notes:
1.  $N(i)$  is index of refraction at atmospheric pressure
  2.  $N(r)$  is index of refraction at shock pressure
  3.  $i$  is angle of incidence ( $45^\circ$ )
  4.  $r$  is angle of refraction
  5.  $\Delta y$  is apparent positional shift due to index of refraction change

Fig. 6. Illustration of Necessary Calculations

where  $\rho_0$  is initial mass density.

Equations 2 - 4 combined express  $\tan(r)$  in terms of  $UP(1)$  and known quantities, and permit Equation 1 to be expressed in terms of one unknown,  $UP(1)$ .

Observed data for L-45 and PMMA at three temperatures are shown in Figs. 7 and 8, where triangles, circles and squares are -45, R.T., and +165 respectively.

Hugoniot relationships for L-45 were derived by first fitting the curves of Fig. 7 to the form  $US = C_0 + B * U(1)$  where  $C_0$  is the speed of sound at atmospheric pressure. Coefficients B and  $C_0$  as well 95% confidence intervals for B are noted in Fig. 7. As may be seen, the confidence intervals overlap, so all data were pooled to yield the following:

$$US = 0.991 \text{ to } 0.940 * U(1) \quad \text{at R.T. } (0 \leq U(1) \leq 5.0) \quad (5a)$$

$$US = 0.825 \text{ to } 0.940 * U(1) \quad \text{at } +165 \text{ F } (0 \leq U(1) \leq 5.0) \quad (5b)$$

$$US = 1.175 + 0.940 * U(1) \quad \text{at } -45 \text{ F } (0 \leq U(1) \leq 5.0), \quad (5c)$$

with a 95% confidence interval for the slopes of  $\pm 0.086$ .

Equation 5 was then used with Equation 2 - 4 to derive smoothed,  $(US, UP)$  - curves by means of Equation 1, as follows:

$$US = 0.991 + 1.88 * UP \quad \text{at R.T. } (0 \leq UP \leq 2.5), \quad (6a)$$

$$US = 0.825 + 1.88 * UP \quad \text{at } +165 \text{ F } (0 \leq UP \leq 2.5), \quad (6b)$$

$$US = 1.175 + 1.88 * UP \quad \text{at } -45 \text{ F } (0 \leq UP \leq 2.5). \quad (6c)$$

Pressure-particle velocity curves for L-45 are shown in Fig. 9; a Hugoniot for distilled water is included for reference. The curves obtained from the form  $P = 10 * \rho_0 * US * UP$  where  $\rho_0$  is initial density. Equation 6 was used for L-45 and

$$US = 1.51 + 1.85 * UP \quad (8)$$

with  $\rho_0 = 1 \text{ gm/cm}^3$ , was used for water.

PMMA-data at three temperatures imply no measurable differences due to thermal environments. These results are reasonable, at least in the low-pressure range, since the speed of sound for PMMA varies little from -45 to +165 F.

Since differences due to temperature were not measurable, the data of Fig. 8 were pooled and a quadratic, least-squares curve fitted, as shown by the solid curve. The quadratic coefficients, relating  $US(1)$  and  $US(2)$  combined with Equations 6 were then used to calculate a smoothed, PMMA Hugoniot with the following results:

$$US = 2.863 + 1.235 UP \quad (0 \leq UP \leq 2.5) \quad (7)$$

which agrees favorably with PMMA-Hugoniots listed in Reference 4.



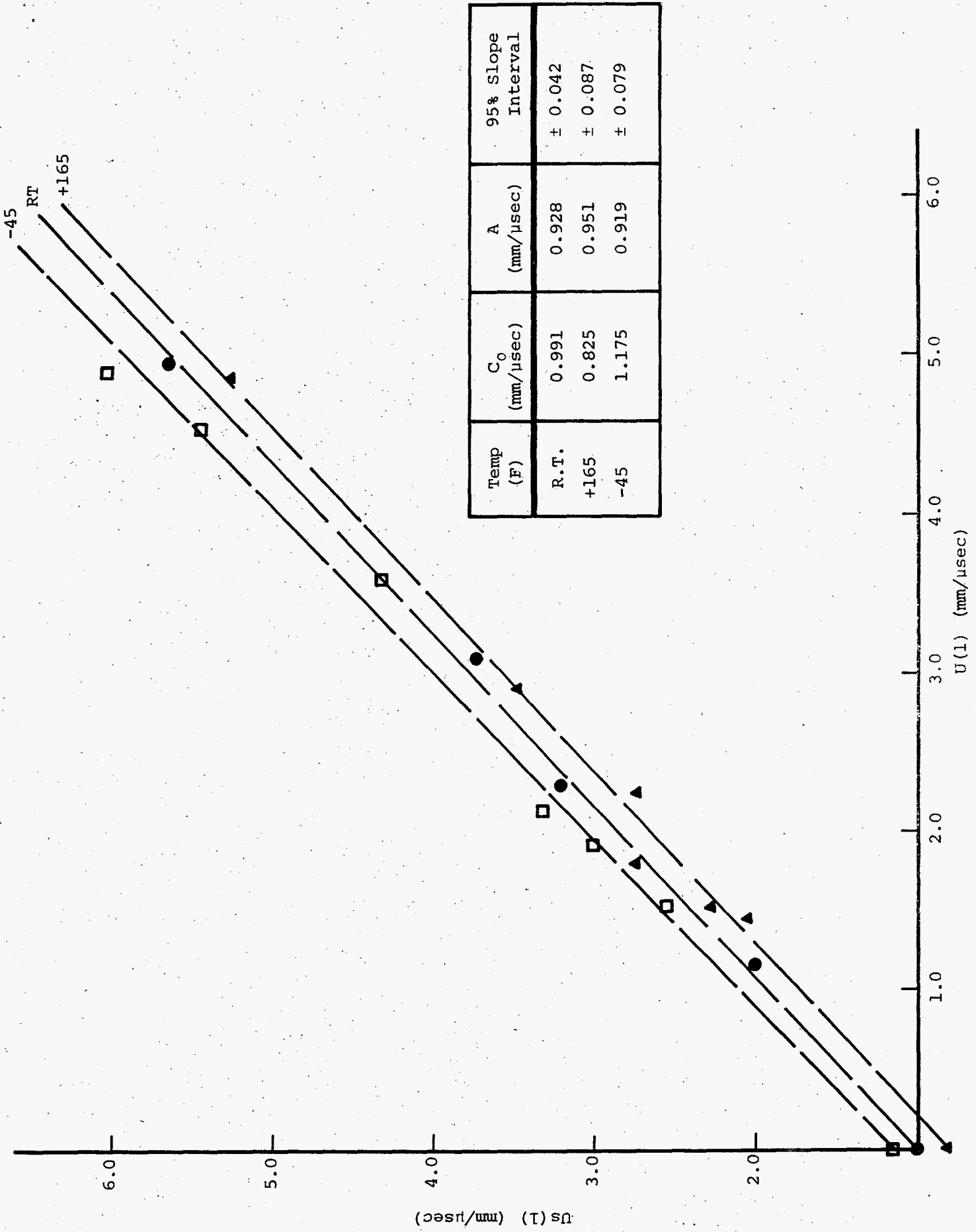


Fig. 7. Measured [U(l), Us(l)]-Data for L-45 at Three Temperatures

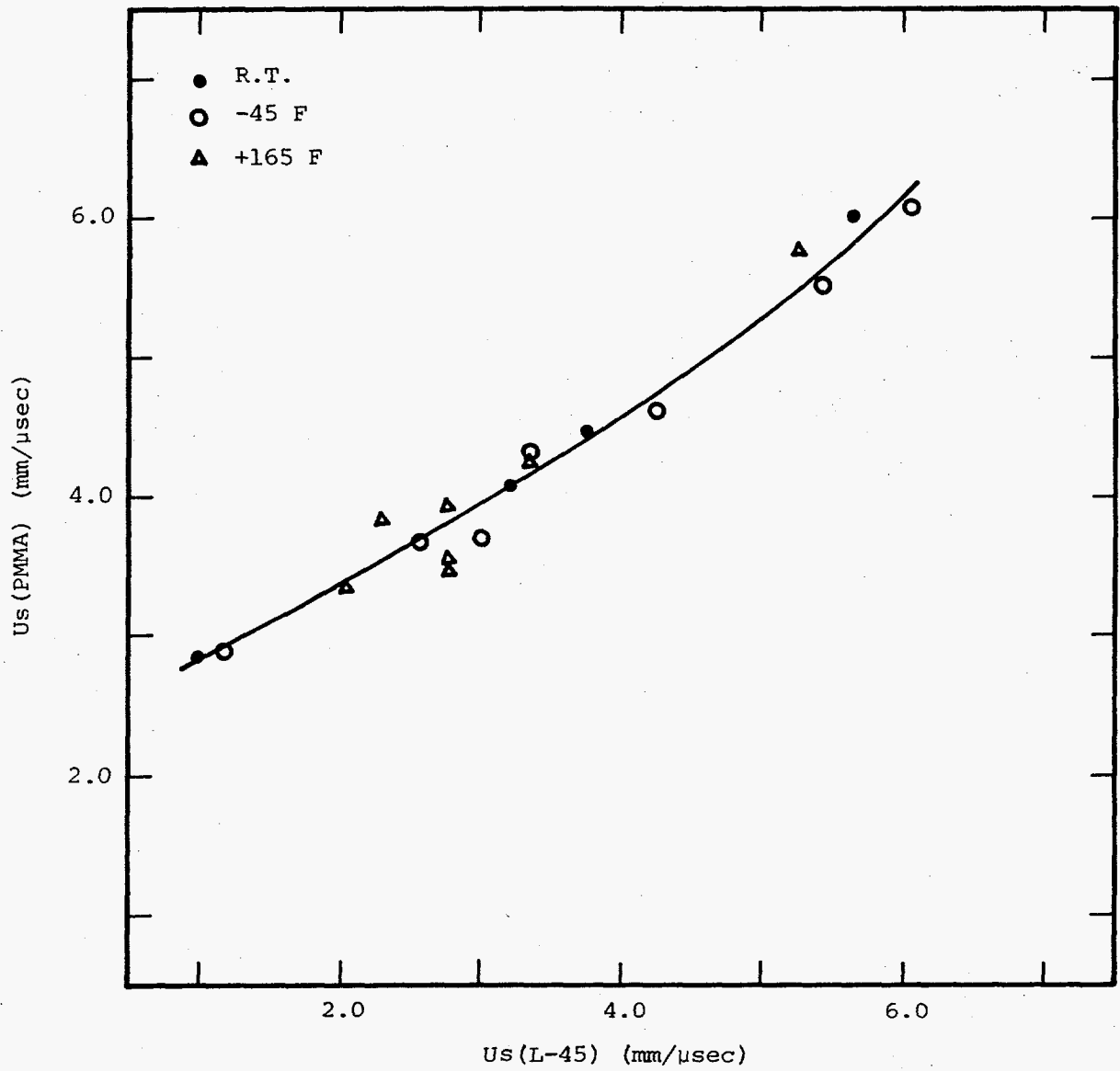


Fig. 8. Shock Velocity Transmitted into PMMA as a Function of Shock Velocity Incident in L-45

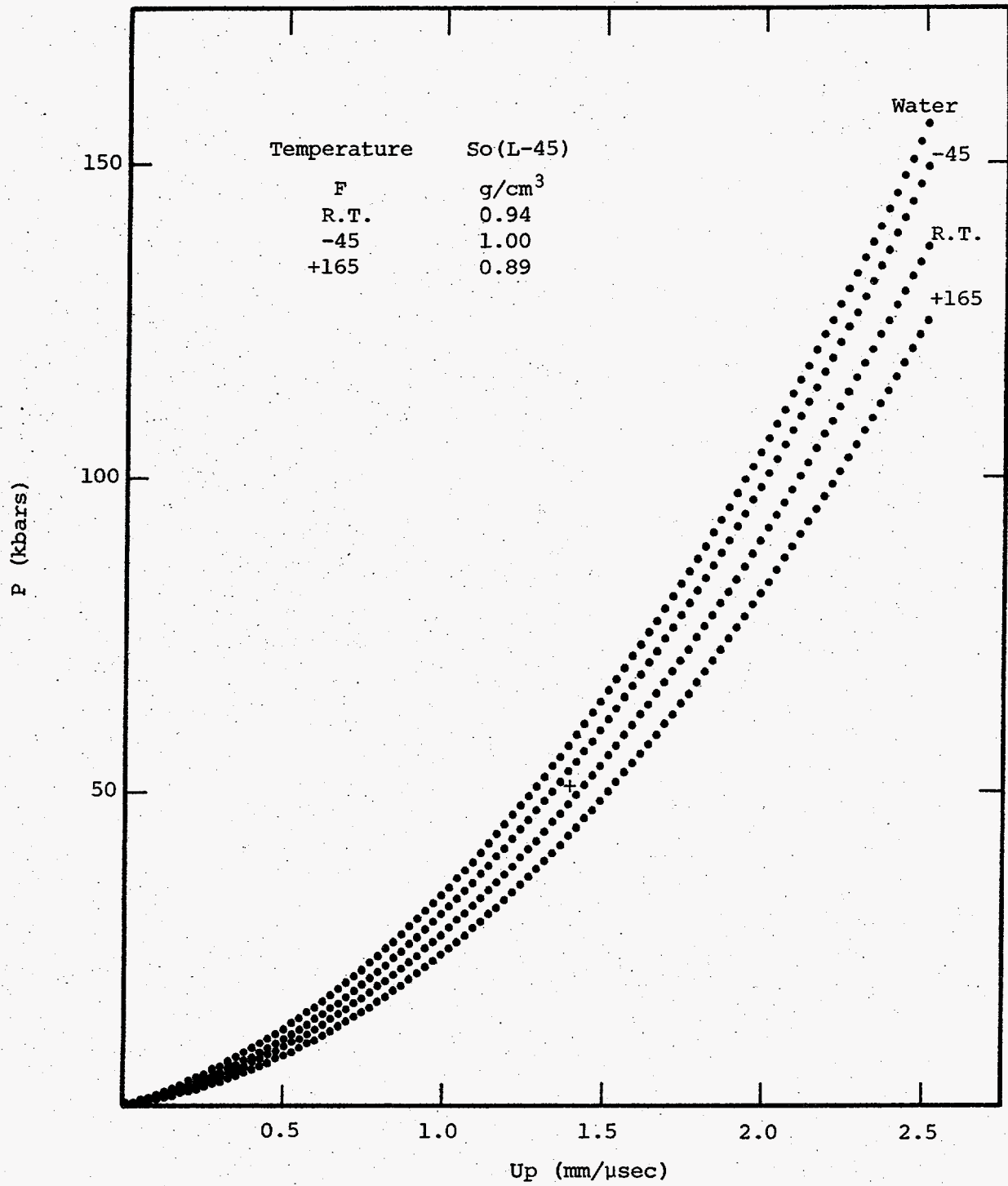


Fig. 9. (P,Up)-Hugoniots for L-45 and Distilled Water

## CONCLUSIONS

Major uncertainties encountered in this project include effects of temperature gradients and applicability of the Gladstone-Dale model.

As may be seen in Fig. 4, temperature differences between the two locations range to 26 F at seven minutes, resulting in a gradient between surface F and C on the order of one degree. Hugoniot information, in theory derivable from surface velocities  $U(2)$  through  $U(5)$ , were not used here due to uncertainties in temperatures associated with their surface locations.

Work is now in progress to characterize the L-45 fluid at -65 F. These tests, however, are being constructed with a vacuum jacket around the aquarium configuration shown in Fig. 2, thereby reducing the maximum temperature decay to less than one degree for the first five minutes.

A test was conducted at room temperature to examine the Gladstone-Dale model. Measured values were  $U_S$  in L-45 and the resultant interface velocity between L-45 and air. The interface velocity, i.e., free-surface velocity was assumed equal to  $2 \times U_P$ . Values obtained were used to calculate the  $(U_P, P)$ -point denoted by the cross in Fig. 9. Agreement between the closed circle and Hugoniot curve are within experimental error and implies applicability of the Gladstone-Dale model to 50 Kbars.

#### REFERENCES

1. Zel'dovich, Ya. B. and Yu. P. Razier, Physics of Shock Waves and High Temperature Hydrodynamic Phenomenon, Academic Press, 1967.
2. Keller. D. V., "Behavior of Short Duration Shocks in Plexiglas", pp. 453-60, Behavior of Dense Media Under High Dynamic Pressure, Symposium H.D.P., I.U.T.A.M., Paris, September 1967, Gordon and Breach, New York, 1968.
3. Handbook of Physics, ed. by E. U. Condon and H. Obishaw, McGraw-Hill Book Company, 1967.
4. Compendium of Shock Wave Data, UCRL-50108 (Vol. 2) ed. by M. Van Thiel, June, 1966.